LAJSBA
LATIN AMERICAN JOURNAL OF SEDIMENTOLOGY AND BASIN ANALYSIS | VOLUME 30 (2) 2023, 95-113

SOIL-GEOMORPHIC RELATIONSHIPS IN A NORTHEASTERN PATAGONIAN TIDAL SALT MARSH, PENÍNSULA VALDÉS, ARGENTINA

Ileana Ríos [1], Pablo J. Bouza [2], Alejandro Bortolus [3], Yanina L. Idaszkin [3], Nicolás Scivetti [2]*

[1] Universidad Nacional de la Patagonia San Juan Bosco. Boulevard Brown 3051, CP U9120 ACF, Puerto Madryn, Chubut, Argentina.
[2] Instituto Patagónico de Geología y Paleontología (CONICET, CCT CENPAT). Boulevard Brown 2825. CP U9120 ACF. Puerto Madryn, Chubut, Argentina. *Corresponding author: bouza@cenpat-conicet.gob.ar
[3] Instituto Patagónico para el Estudio de los Ecosistemas Continentales (CONICET, CCT CENPAT). Boulevard Brown 2825. CP U9120 ACF. Puerto Madryn, Chubut, Argentina.

ARTICLE INFO

Article history
Received June 22, 2023
Accepted October 4, 2023
Available online October 25, 2023

Handling (guest) Editor
Alfonsina Tripaldi

Keywords
Pyrite framboids
Potential acid sulfate soils
Carbon stable isotopes

ABSTRACT

Salt marsh ecosystems have been studied extensively based on the interaction between geo-morphological and geo-ecological processes, but a soil-geochemistry approach is currently unknown in Patagonia. This work was conducted in Riacho salt marsh (Patagonia, Argentina), to establish the soil-geomorphology relationship with a focus on geochemical analysis and vegetation changes (C3 vs. C4 photosynthesis pathway plants). The geochemical analysis was focused on sulfidic material occurrence and their potential acid generation, while the vegetation-geomorphology relationship was determined through the $\delta^{13}C$ composition from soil organic matter. To achieve this, soil descriptions and laboratory analyses of soil samples were performed. Riacho salt marsh soils correspond to the Entisol Order and the Suborder Aquents. Soils corresponding to *Sarcocornia perennis* and *Limonium brasiliense* vegetation units were classified as Sodic Hydraquents, which were associated with tidal flats occurring between Holocene beach-ridges systems. On the other hand, the soil corresponding to the *Spartina alterniflora* vegetation unit was classified as Haplic Sulfaquents related to salt marsh lower levels, where waterlogging soil conditions favor the sulfidic materials formation. These soils are considered potential acid sulfate soils due to the generation of sulfuric acid by oxidation processes. Consequently, extreme oxidation of these soils could release metals. The $\delta^{13}C$ isotope composition of soil organic matter, in combination with the C/N ratio, indicates that the sandy C horizons from soils corresponding to high salt marsh levels would constitute pioneer salt marshes, which is consistent with the Holocene salt marshes development. The plant zonation model responds to the ecological succession according to the geomorphological evolution. Future isotopic studies will be necessary to determine the contributions of different sources, both surface runoff of organic matter from continental ecosystems and organic matter from marine origin.

INTRODUCTION

Salt marsh ecosystems worldwide occupy about 0.20 to 0.40 million km^2 on Earth (Nellemann *et al.*, 2009; Laffoley and Grimsditch, 2009). They constitute refuge and breeding areas for a variety of animals, and are also recognized as the most productive ecosystems on Earth due to their high primary productivity (Adam, 1993; Mitsch and Gosselink, 1993; 2000).

Salt marsh vegetation is composed of halophyte plants tolerant to partial immersion and edaphic hypersalination that could be arranged in a specific distribution pattern (zonation). This non-random pattern is composed of patches or stripes interrelated with the immersion and edaphic and tidal properties (Álvarez-Rogel *et al.*, 2001; Idaszkin *et al.*, 2011), and with ecological interactions such as competition or inter and intra-species facilitation (Pennings and Callaway, 1992; Bertness and Shumway, 1993; Adam, 1993; Idaszkin *et al.*, 2011; Li *et al.*, 2018). This pattern also could reflect ecological succession assuming that bare tidal flats are colonized by typical low marsh species tolerant to both salinity, immersion, and anoxia, as C4-type plants. These plants promote soil accretion by trapping sediment and raising the surface. This, in turn, enables the colonization of other species in the newly formed high marsh, including C3-type plants. Eventually, the first colonizing plants would disappear (Leeuw *et al.*, 1993), possibly settling in the new lower levels of the marsh. However, changes in vegetation may also be due to changes in sea level, continental water, and sediment discharges or any other possible event (*e.g.*, storminess) or geomorphological and sedimentological processes (*e.g.*, changes in depositional regimes and sediment autocompactation) which took place during Holocene (Choi *et al.*, 2001; Lamb *et al.*, 2006, 2007).

One way to determine these changes through the soil profile is by assessing the proportion of C4/C3 plants through $\delta^{13}C$ isotopic compositions from soil organic matter (Chmura and Aharon, 1995; Choi *et al.*, 2001; Lamb *et al.*, 2006, 2007). This is based on the discrimination of CO_2 by plants during photosynthesis, which is influenced by the biochemical properties of primary enzymes involved in carbon fixation and the diffusion process that regulates CO_2 entry into leaves (Farquhar *et al.*, 1989). This type of discrimination varies according to the photosynthetic cycles of terrestrial plants, namely C3, C4, and CAM. C3 plants reduce CO_2 to phosphoglycerate (3C) via the ribose bisphosphate/oxygenase enzyme (Rubisco). That is why the plants with this type of photosynthesis have a $\delta^{13}C$ of -32 ‰ to -22 ‰ with an average of -27 ‰ (Boutton, 1991). They are best adapted to cool and wet environments. In contrast, C4 plants utilize the enzyme phosphoenolpyruvate carboxylase (PEP) to convert CO_2 into aspartic or malic acid (4C). These plants show less discrimination against $^{13}CO_2$, resulting in higher $\delta^{13}C$ values compared to C3 plants. The isotopic range for this plant type is -17 ‰ to -9 ‰ with an average of -13 ‰. (Boutton, 1991). They are well-suited for hot and sunny environments, which confers an evolutionary advantage to C4 plants in the context of global warming (Hattersley, 1983; Ehleringer and Cerling, 2002).

The soils of salt marshes experience periodic tidal flooding and waterlogging, leading to saturation in certain parts of the soil profile. As a result, these soils often do not exhibit extensive pedologic development and are commonly classified as Aquent Suborder (Soil Survey Staff, 1999). Additionally, the high salt content and reducing conditions in these soils create favorable conditions for the occurrence of sulfidic materials, classified as the Great Group of Sulfaquents. One of the most outstanding features of these environments is that they present the optimum conditions for sulfides formation in sediments, such as the presence of Fe-rich sediments, the seawater sulfate, and the removal of reaction products (*i.e.*, bicarbonates), the presence of sulfate-reducing bacteria, and the amount of organic matter (Ahern *et al.*, 1998). Thus, pyrite (FeS_2) is the most frequent sulfidic mineral that is formed according to the following equation:

$$Fe_2O_3(s) + 4SO_4^{2-} + 8CH_2O + 1/2\ O_2 \rightarrow 2FeS_2(s) + 8HCO_3^- + 4H_2O \quad (1)$$

As a result, bicarbonate is removed from the sediments, leaving pyrite as a potential source of acidity (Giblin, 1988; White *et al.*, 1997). Particularly, the formation and oxidation processes of these reduced Fe compounds are one of the most important and complex oxidation-reduction reactions that occur on salt marshes and are an Eh and pH-dependent process. Thus, the presence of sulfidic material can generate a pH decrease when they are

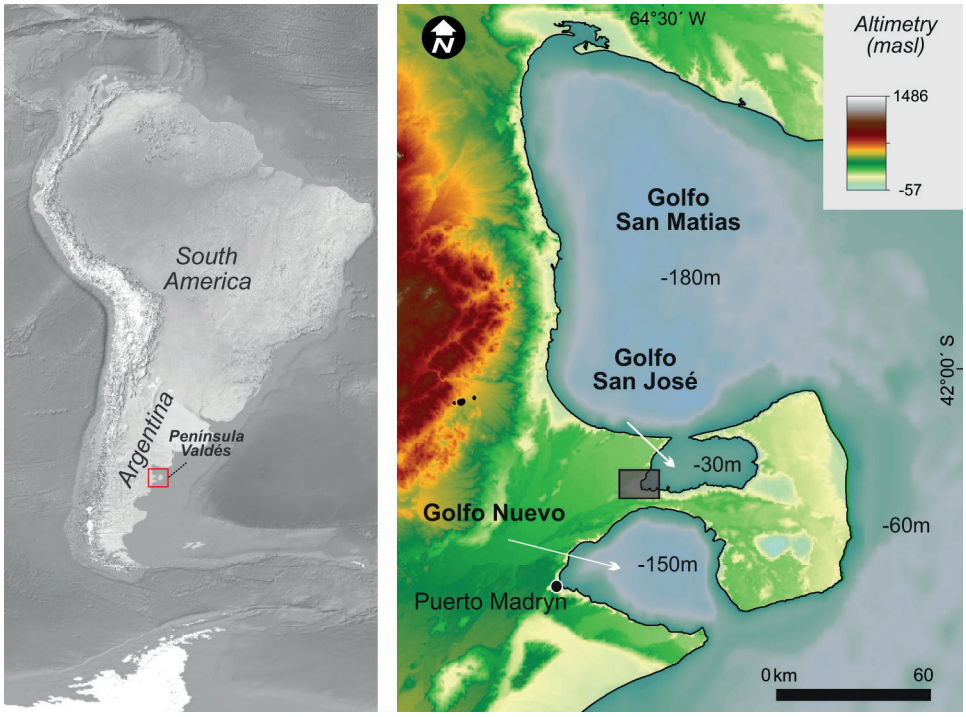

Figure 1. Map showing the location of the study site: Riacho salt marsh (42, 43° S, 64, 61° W) in Peninsula Valdés area, Patagonia, Argentina.

oxidized, according to the following equation (Van Breemen, 1982):

$$FeS_2 + 15/4\ O_2 + 7/2\ H_2O \rightarrow Fe(OH)_3 + 4H^+ + 2SO_4^{2-} \quad (2)$$

If the pH <3 and the solution contains iron ions, the oxidation occurs in the absence of O_2 producing 16 H^+ equivalents:

$$FeS_2 + 14Fe^{3+} + 8H_2O \rightarrow 15Fe^{2+} + 16H^+ + 2SO_4^{2-} \quad (3)$$

During oxidation processes (eqs. 2 and 3), two types of precipitates can be formed in these environments. Firstly, combinations of iron and oxygen can result in the formation of iron oxides or hydroxides such as goethite, hematite, and amorphous oxyhydroxides like ferrihydrite. Secondly, combinations of sulfates and iron can lead to the formation of jarosite [$(Na^+, K^+, NH_4^+, H_3O^+)Fe_3(SO4)_2(OH)_6$] and melanterite ($FeSO_4{\cdot}7H_2O$).

Extensive research on salt marshes on the Extra-Andean Patagonian coasts has been performed over the years (Bortolus *et al*., 2006, 2009; Idaszkin and Bortolus, 2011; Idaszkin *et al*., 2011, 2014, 2015, 2017, Bouza *et al*., 2019). Regarding the pedology and geomorphology approach, Bouza *et al*. (2008) conducted a preliminary study describing salt marsh soils and classified the main Patagonian salt marshes. In addition, research on the Riacho salt marsh has only been focused on multi-disciplinary studies with ecological and economic interests (Idaszkin *et al*., 2011; Bocco *et al*., 2013). Moreover, integrated studies on soil-geomorphology relationships and geo-ecology are scarce, mainly those aimed at elucidating landscape evolution, ecological processes, and geochemical processes (Ríos, 2015; Ríos *et al*., 2018).

Therefore, this study aims to establish the soil-geomorphology relationship in the Riacho salt marsh to identify sulfidic materials and determine the succession vegetation dynamics associated with the landscape ecology pattern. These results will substantially increase the knowledge about salt marsh soils and eco-geomorphology and will be useful in developing management strategies.

STUDY AREA

This study was performed in the Riacho salt marsh situated at 42º 24' 46" S, 64º 37' 29" W in Chubut province, Argentina, on the west coast of the Golfo San José (Fig. 1). The study area is located mainly in a coastal transition climate region, approximately between the 41º and 43º parallels of

latitude. This region encompasses both the Monte and Patagónica phytogeographic provinces (Cabrera, 1976), as well as the Argentine and Magellan marine zoogeographic regions (Boschi, 1979; Menni and Gosztonyi, 1982). The Golfo San José has a subelliptic shape and constitutes the smallest gulf on the North Patagonian coast (814 km^2). Its average depth is 30 m (maximum 80 m) and is linked with the Golfo San Matías through a 6.7 km wide mouth. These particular characteristics produce differences between the eastern and western areas of the gulf through the distribution of the tidal streams entering and leaving their mouth (vortex dipoles or mushroom currents, Amoroso and Gagliardini, 2010).

The climate in the study area is temperate-arid with a marked climatic gradient from east to west with an average annual rainfall of less than 200 mm –presenting an autumn-winter regime with a 225 mm annual average– that gives it the conditions of aridity, but, in the sector where it is framed Península Valdés, these characteristics are attenuated by the influence of the sea (Coronato, 1994). The mean annual temperature is 14 ºC with great thermal amplitude (Coronato *et al.*, 2017). Winds dominate from the west and southwest quadrants with an average speed of 22 km h^{-1}. The hydrological regime is mesotidal, reaching the highest tide values of 8.2 m a.s.l.

According to the classification proposed by Pye and French (1993), Riacho salt marsh is classified as a restricted-entrance embayment, characterized by a sandy-loam sediment grain size, and protected from the wave action by sandy-gravel barrier spits and barriers (Bouza *et al.*, 2008). One of the most outstanding geomorphic features of Riacho salt marsh is the wide extension spits that run in the SE-NW sense belonging to the San Miguel Formation (Middle Holocene, Haller, 1981, 2017), which is mainly composed of medium to coarse gravel, with a matrix of fine gravel, coarse sand, and fragments of bivalves. In that regard, three systems of gravel spits were dated on mollusk shell-fragments by radiocarbon-14 as follows in declining age (Fig. 2): I (6290 ± 90 years), II (2405 ± 70 years, and III (1140 ± 50 years) (Weiler, 1998).

The dominant plants in the Riacho salt marsh belong to the genus *Spartina* (Bortolus *et al.* 2019). Specifically, *Spartina alterniflora*, which is tolerant to soil anoxia, is found at the lowest and permanently flooded level of the salt marsh. On the other hand, *Spartina densiflora*, *Limonium brasiliense*, and *Sarcocornia perennis* thrive at the highest level of the salt marsh (Bortolus *et al.*, 2009; Idaszkin *et al.* 2011).

Related to conservation, the Riacho salt marsh, like all Península Valdés wetlands, was included in 2012 in the RAMSAR convention list for conservancy (Committee on Characterization of Wetlands, 1995).

MATERIALS AND METHODS

Fieldwork

The landform elements and the main vegetation units were delimitated by aerial photographs (1:20,000; Servicio de Hidrografía Naval Argentina) and satellite images from Google Earth ™.

To assess the influence of tidal stages, Sentinel-2 satellite images from March 22, 2022, with a resolution of 20 meters per pixel, were used to analyze the patterns of suspended sediments, which serve as indicators of turbulent flows. It was carried out using the normalized difference turbidity index (NDTI) (Lacaux *et al.*, 2007), which is useful for detecting turbid water. The value of this index ranges from −1 for turbid water to +1 for clear water.

Soil profiles were made in each landform associated with the typical vegetation dominated by the marsh, including *Spartina alterniflora* (Sa soil), *Limonium brasiliense* (Lb soil), and *Sarcocornia perennis* (Sp soil).

Soil sampling was made considering the water table as the profile bottom limit. Soil horizon designation, morphological description, and soil sampling were performed according to Schoeneberger *et al.* (2012). To characterize the geochemical environment, the field pH (pHf) and redox potential (Eh) of each soil horizon were determined by using an electrode of a portable digital pH/Eh-meter according to the procedure of Faulkner *et al.* (1989). All the samples were pocketed in PVC bags and stored in coolers at 4° C for transport.

Laboratory procedures and analytical determinations

Incubation pH is used to test for the presence of sulfidic material and to predict the occurrence of potential acid-sulfate soils. The presence of sulfidic material (oxidizable sulfur compounds) is used as a criterion for soil classification (*e.g.*, Sulfaquents).

Figure 2. Geomorphological sketch of the Riacho salt marsh based on satellite image and field controls. I-IV: Complex beach-ridge systems defined by Weiler (1998)

Soils are considered potential acid-sulfate soils if the sulfide material is waterlogged mineral, organic, or mixed soil material with a pH of 3.5 or higher and, if incubated as a 1-cm thick layer under moist, aerobic conditions (field capacity) at room temperature, shows a pH drop of 0.5 or more units to a pH value of 4.0 or less within 16 weeks or longer, if the pH is still dropping after 16 weeks until the pH reaches a nearly constant value (Soil Survey Staff, 2014).

In the laboratory, a part of the soil samples was immediately separated to determine the occurrence of sulfidic minerals through the incubation pH (pHi).

The presence of potential acid sulfate soils was also assessed by the potential oxidation technique, in which pH is recorded after complete soil oxidation with hydrogen peroxide 30% (pHp), adjusted to pH 5 (Ahern *et al.*, 1998). Then the rest of the soil sampled was separated into two fractions: one was stored in a freezer at -20 ºC and another was used to perform analytical determinations. To do this, samples were air-dried and sieved to separate the gravel (> 2mm) from the finest material (< 2mm); and estimate its percentage. On the other hand, frozen samples were heated in a stove up to 85 °C to destroy sulfur-oxidizing bacteria (Lin and Melville, 1993) and then sieved at 2mm mesh size. The particle size distribution (USDA system) was determined by the hydrometer method (Bouyoucos, 1927). The pH and electrical conductivity (EC) were determined in a soil-water extract 1:2.5. Soluble salts in those extracts were also determined: Ca^{2+} and Mg^{2+} by titration with EDTA; Na^{+} and K^{+} by flame spectrometer; Cl^{-} by qualification with silver nitrate and SO_4^{2-} by electrical conductivity (U.S.

Salinity Laboratory Staff, 1954). The cation exchange capacity (CEC) was determined by the saturation of the samples with Na^+ 1N acetate at pH 8.2. The exchangeable Na^+ was extracted with acetate-NH_4^+ 1N at pH 7 and it was subsequently measured with a flame spectrophotometer. The total nitrogen (N) was determined by the micro-Kjeldahl method and the soil organic matter was determined by ignition at 430 ºC, and previous drying of the sample at 105 °C (Davies, 1974). The soil organic carbon (C) content was determined by dividing the soil organic matter (SOM) content by factor 1.72 (Page *et al*., 1982).

The calcium carbonate equivalent was measured by the gravimetric method (U.S. Salinity Laboratory Staff, 1954). The sodium adsorption ratio (SAR) and exchangeable sodium percentage (ESP) were calculated from soil soluble salt concentration as follows:

$$SAR = [Na^+ / (Ca^{2+} + Mg^{2+})^{-2}]^{1/2}$$

$$ESP = [(-0.0126 + 0.0145 \cdot SAR)^{-1} + (-0.0126 + 0.0145 \cdot SAR)]$$

Soil classification was made according to Soil Taxonomy (Soil Survey Staff, 2014). In this order, the *n* value, an index that establishes the relationship between the water percentage at field conditions and the clay and SOM percentage, was calculated as follows:

$$n \text{ value} = [(A - 0.2\ R) \cdot (L + 3H)^{-1}]$$

where:

A: % H_2O. R: % silt + clay L: % clay H: % SOM

On the same soil samples, a Jeol JSM 6460 LV scanning electron microscope with an EDAX PW7757/78 X-ray energy-scattering micro-analyzer (SEM-EDS) and a Zeiss Supra 40 scanning electron microscope with EDS Oxford Instruments were used to examine the morphology of sulfidic and oxidized materials after incubation and to determine the composition of certain soil particles.

As regard C3 and C4 proportion, the $\delta^{13}C$ isotopic composition was determined in soil organic carbon and leaf tissues by putting between 2000 and 8000 μg sample grounded at 0.5 mm sieve (40-mesh) and pre-treating with HCl to remove the inorganic carbon in tin capsules. Leaf plant tissues of *S. alterniflora*, *L. brasiliense,* and *S. perennis* were field harvested and laboratory cleaned in an ultrasonic bath and oven-dried at 40 °C. The grounded samples were analyzed in an elemental analyzer (Carlo Erba EA1108) coupled to a mass spectrometer continuous flow isotope ratio (Termo Scientific Delta V advantage) through a Conflo IV interface. The $\delta^{13}C$ values were normalized in the L-SVEC-NBS-19 scale, according to Coplen *et al*. (2006). The abundance of C4 plants in modern vegetation was estimated by the isotopic composition of the SOM (Weiguo *et al*., 2003) as follows:

$$\delta^{13}C_{soil} = \delta^{13}C_{C4} f + \delta^{13}C_{C3} (1-f)$$

The f is the relative abundance of C4 plants in the vegetation, and (1- f) is the relative abundance of C3 plants in the vegetation. The natural abundance of $\delta^{13}C$ in plants was taken from Carvajal *et al*. (2013), wherein C3 vegetation is -26‰ (e.g., *S. perennis* and *L. brasiliense*) and C4 vegetation is -12‰ (e.g., *Spartina sp*.)

Finally, the C/N ratio was used to establish if the origin of organic matter was autochthonous (C/N>12) or allochthonous (Tyson 1995; Lamb *et al*., 2006, Lamb *et al*., 2007).

RESULTS

Geomorphology

The restricted-entrance embayment salt marsh is shown in Figure 2, where a complex beach-ridge system (spit system) dominates in the intertidal area. Beach-ridges Systems I-III have a SE-NW predominant direction and are covered by the typical vegetation of the Patagonian steppe, as well as *Atriplex vulgatissima*, *Franquenia juniperoides*, and *Larrea nitida* (Fig. 3a). While System IV presents a near S-N trend and it is composed by bare soil.

Between the piedmont slope and the beach ridges of System I, a salt pan that corresponds to a paleo coastal lagoon occurs. In this area, next to de beach ridge System I, a paleo-salt marsh is observed (Fig. 3a), recognized by the presence of redoximorphic features, mainly reddish brown rhizoconcretions (5YR 4/4, redox concentrations, Fig. 3b) embedded in a grayish olive gley soil matrix (5Y 5/2, redox depletions, Fig. 3c).

Beach Ridge Systems II and III are surrounded by high and low marsh levels, where the soil has a

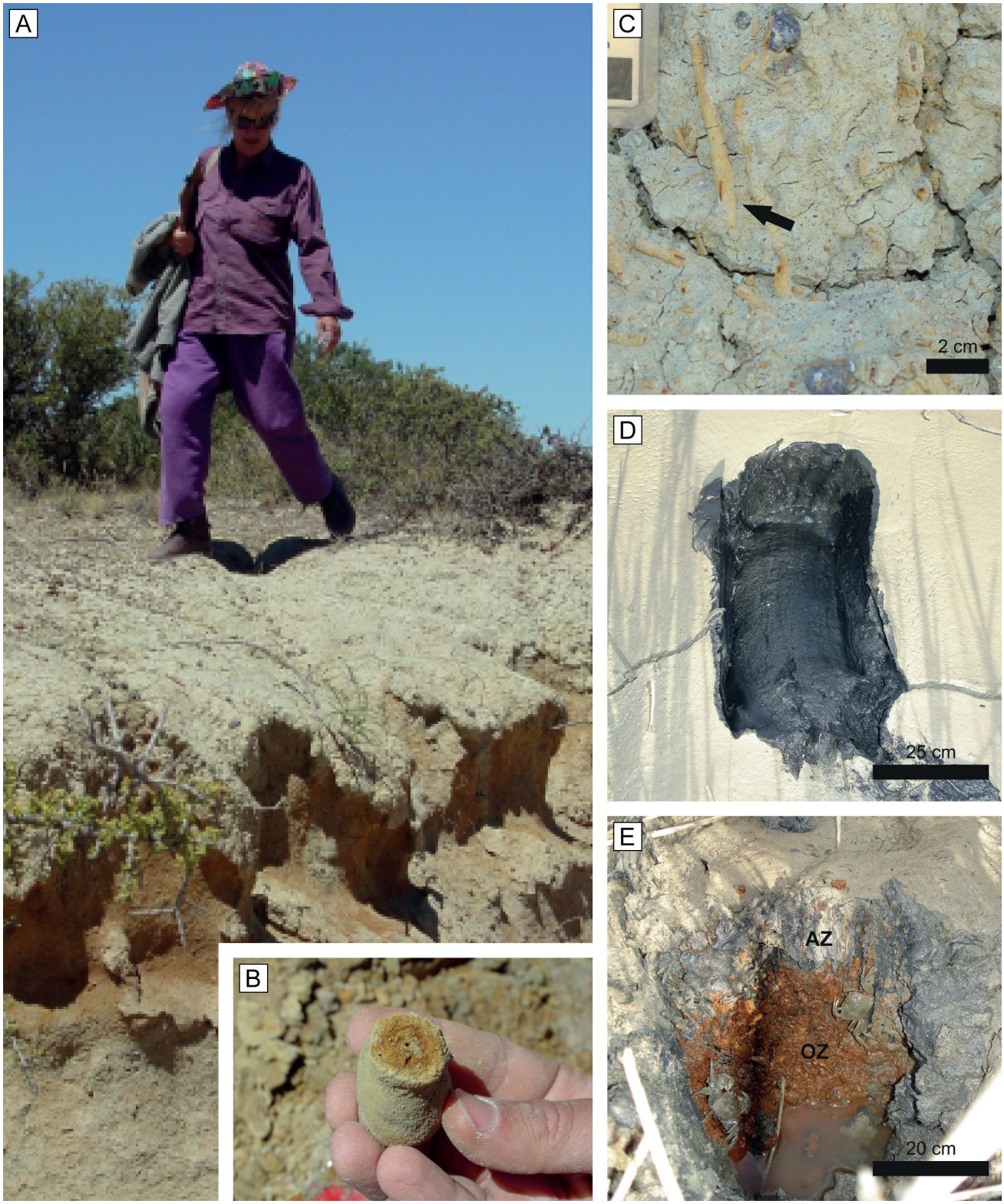

Figure 3. Morphology and redoximorphic characteristics. **a)** Beach Ridge System I and paleo-salt marsh associated, **b)** reddish brown rhizoconcretion (black arrow), **c)** redoximorphic features, redox concentrations (*e.g.*, rhizoconcretions, 5YR 4/4) and redox depletions (grayish olive gley soil matrix, 5Y 5/2), **d)** surficial anoxic clayed sediment, **e)** inverted redox pattern in low salt marsh physiographic positions: anoxic fine surficial sediments (anoxic zone, AZ) on oxic sub-surficial gravelly deposit (oxic zone, OZ).

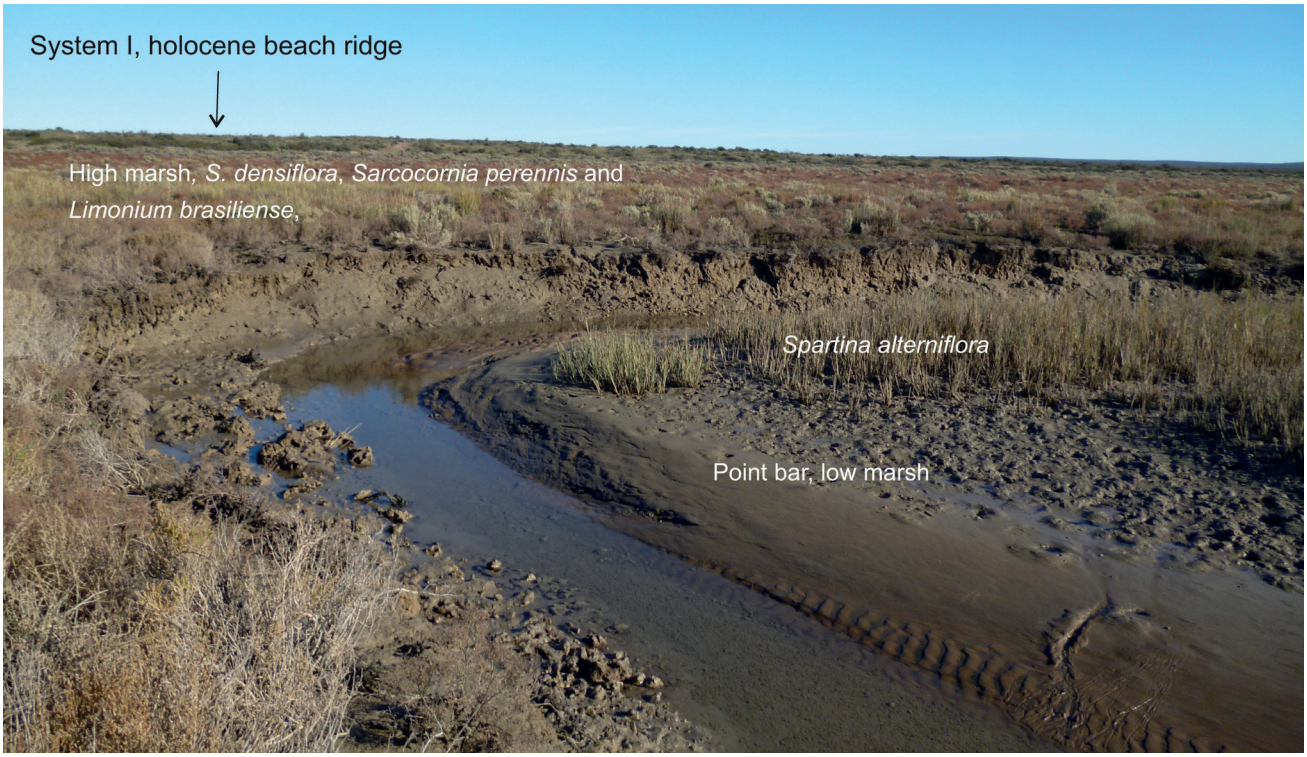

Figure 4. Physiographic positions of the Riacho salt marsh: distribution of plant communities and geomorphic characteristics.

predominantly silt loam texture. In general, when sediments have uniform textures, the reduction pattern increases in depth and below the fluctuation zone of the water table, except when the salt marsh develops above the gravelly beach ridges, where the interstitial waters contain more dissolved oxygen and therefore have greater redox potential (Eh > 0). This creates an inverted redox pattern, where the fine surficial sediments are anoxic (Eh < 0), while the sub-surficial gravelly deposit is oxygen-rich (Fig. 3d, f).

The low salt marsh level is associated with both point bars of the tidal channels and mud and sand flats. The low salt marsh is colonized by *Spartina alterniflora* (Sa, C4 plant), while the high marsh level is colonized by *S. densiflora* (C4 plant), *Sarcocornia perennis* (C3 plant), and *Limonium brasiliense* (C3 plant) (Fig. 4).

Soils and landscape relationships

Soil profiles associated with landforms and vegetation pattern is indicated in Figure 2, while their physical and chemical properties are shown in Table 1.

The *Spartina alterniflora* soil profile (Sa soil) is developed on tidal plains, where the daily flood regime covers the entire extension of this vegetation unit zone, which is favored by the presence of numerous tidal channels. The water table level at the time of soil description was above 109 cm depth. The horizon sequence was: Ag-Cg1-Cg2-Cg3-2Cg4 (Fig. 5a) with predominantly silt loam texture and an *n*-value < 0.7. The presence of black mottles (7.5 YR 2/0) and abundant rhizomes in the Ag horizon was observed. Redoximorphic pedofeatures are composed of reddish mottles (5 YR 4/6) observed in Cg1 and Cg2 horizons. Additionally, abrupt changes in Eh from C1g and 2Cg4 horizons were observed (Table 1).

The *Limonium brasiliense* soil profile (Lb soil) was located on the northwest side of the System II gravel spit. The sequence of horizons was: A1-A2-C1-2C2-3C3-4C4 (Fig.5b), with silt loam texture in the upper soil horizons, while below lithological discontinuity, the gravel content increased and the soil is sand texture. The water table at the time of description was 122 cm deep and the *n*-value was > 7. Yellowish brown (10 YR 5/4) and dark reddish brown iron oxide concretions were found in the C1 and 3C3 horizons, respectively.

Pedons	Depth	Color (moist)	Structure [a]	Boundary [b]	Gravel	Sand	Silt	Clay	Eh	pHf	pHi	pHp	$CaCO_3$	C	N	C/N	$\delta^{13}C$
Horizons	(cm)	matrix – mottles					(%)		(mV)	field	inc.	peroxide		(%)			(‰)
(Sa)	Spartina alterniflora soil, Haplic Sulfaquents																
Ag	0-20	5Y 3/2- 7.5 YR 2/0	m	gs	0.9	3.8	79.6	16.6	-279	7.46	4.95	2.43	0.7	12.89	0.85	15.2	-16.7
Cg1	20-44	5Y 3/2- 5YR 4/6	m	gs	0.0	4.3	79.2	16.5	-4	7.20	3.51	1.86	0.6	14.38	0.90	16.0	-14.3
Cg2	44-64	5Y 3/2- 5YR 4/6	m	gs	0.0	2.3	79.7	18.0	-182	7.27	5.44	1.94	0.5	14.66	1.14	12.8	-16.7
Cg3	64-138	5Y 3/1	m	gs	0.0	3.0	82.0	15.0	-348	7.25	3.92	2.14	0.7	8.77	nd	nd	-14.8
2Cg4	>138	5Y 4/1	sg	-	0.0	76.6	15.8	7.6	-97	7.66	4.33	2.67	0.9	1.26	nd	nd	-15.9
(Lb)	Limonium brasiliense soil, Sodic Hydraquents																
A1	0-8	10 YR 3/4	gr	as	0.4	13.7	78.7	7.6	146	7.93	7.94	5.22	0.6	7.30	0.35	20.9	-20.1
A2	8-20	10 YR 5/4	sbk	gw	0.8	18.6	60.6	20.8	200	7.48	7.52	4.95	0.6	4.20	0.21	19.7	-18.4
C1	20-60	5 YR 5/2 -10 YR 5/4	-	as	1.6	16.2	72.5	11.3	222	7.39	7.19	5.68	0.6	3.35	0.13	26.4	-17.1
2C2	60-70	5 YR 5/2	sg	as	65.2	87.8	7.2	5.0	290	7.29	7.32	6.57	0.3	1.43	0.08	17.7	-17.2
3C3	70-92	5 YR 3/3	sg	gs	71.0	87.8	8.2	4.0	286	7.29	7.38	5.52	0.3	1.85	0.13	13.9	-18.5
4C4	>92	7.5 YR 4/4	sg	-	82.0	90.7	3.8	5.5	286	7.32	7.29	5.78	0.4	1.69	0.12	13.9	-17.5
(Sp)	Sarcocornia perennis soil, Sodic Hydraquents																
A	0-17	10 YR 3/4	m	gs	0.0	3.6	69.4	27.0	96	6.95	7.25	4.21	0.5	6.91	0.48	14.4	-22.2
C1	17-31	10 YR 4/4	m	gs	16.3	39.1	42.9	18.0	164	6.92	7.01	5.43	0.5	2.72	0.85	3.2	-19.8
2C2	31-43	10 YR 4/4	sg	gs	58.9	76.5	4.5	19.0	191	6.81	7.04	6.74	0.3	1.20	0.07	17.7	-19.8
2C3	43-52	10 YR 3/4	sg	gs	1.6	92.6	0.0	7.4	208	6.82	7.40	5.42	0.2	0.65	0.05	13.3	-19.6
3Cg	52-67	5Y 7/2	sg	gs	12.1	71.4	13.0	15.6	239	6.76	6.73	5.68	0.3	0.88	0.04	19.7	-20.1
4Co	67-82	10 YR 5/4- 5YR 4/4	sg	as	71.4	94.0	1.9	4.0	240	6.96	7.09	6.50	0.3	0.93	0.05	17.0	-20.9
5C	>82	10 YR 4/4	sg	-	46.1	98.9	0.0	1.1	175	7.15	7.18	6.15	0.3	0.16	0.01	15.6	nd

Table 1. Physical and chemical properties of Riacho salt marsh soils.

[ab] Abbreviations for morphological description are from Schoeneberger *et al*. (2012); structure: *gr* granular, *sg* single grain, *m* massive, *sbk* subangular blocky; boundary: distinctness: *a* abrupt, *g* gradual; topography: *w* wavy, *s* smooth; nd not determined

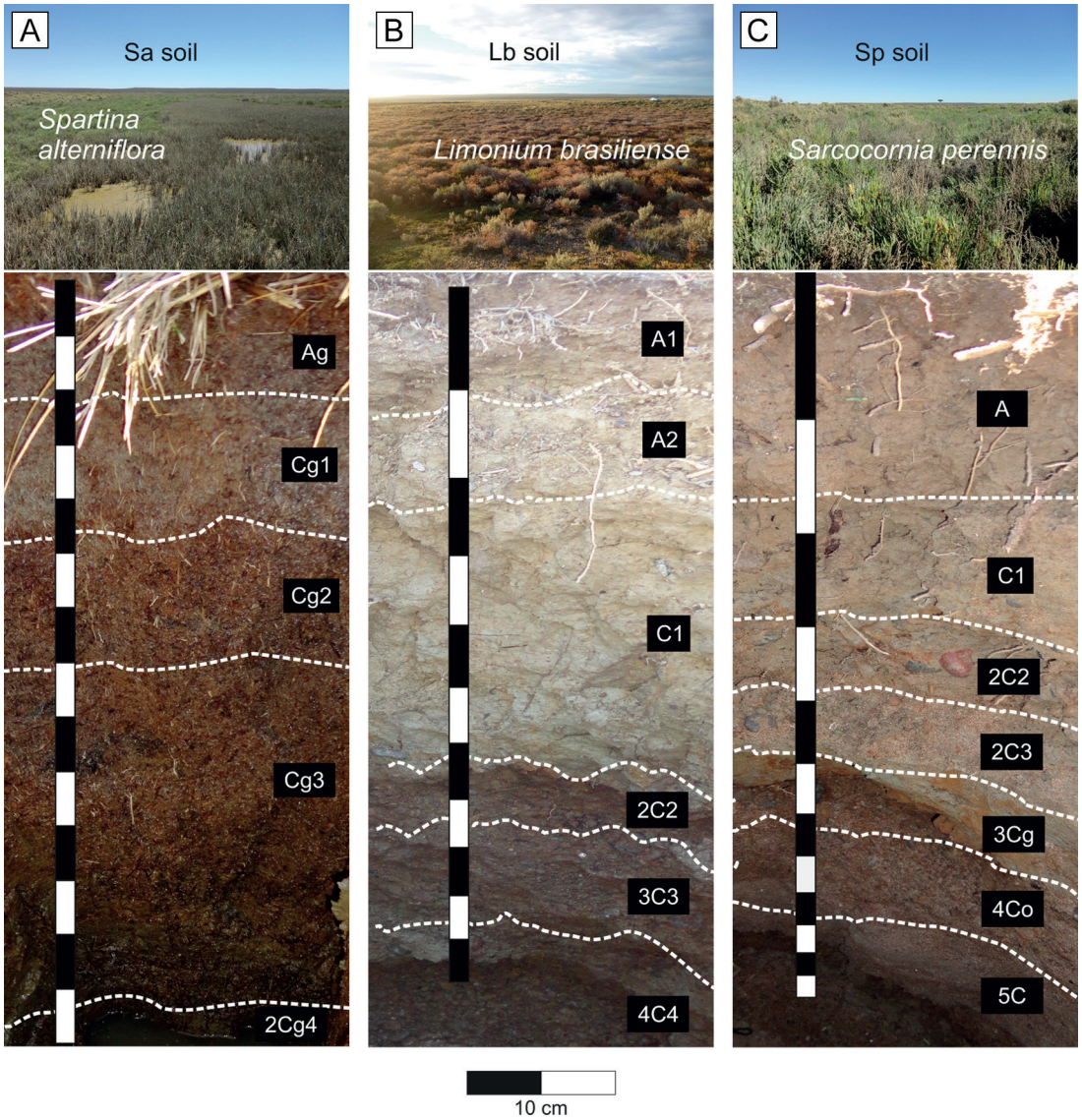

Figure 5: Riacho salt marsh soil profiles, a) Soil of the *Spartina alterniflora* community (Sa soil); is noted to have abundant redox concentrations due to rhizomes activity (reddish color). b) Soil of *Limonium brasiliense* community (Lb soil), the lithologic discontinuity between surficial fine soil parent material and gravelly deposits from buried Holocene beach ridge is observed. c) The soil of the *Sarcocornia perennis* community (Sp soil) has different sizes of gravel through profile characterize it.

The *Sarcocornia perennis* soil profile (Sp soil) is developed between Systems I-III beach ridges. The horizon sequence was A-C1-2C2-2C3-3Cg-4Co-5C and the water table at the time of description was about 109 cm depth (Fig. 5c). The upper soil horizons exhibit variations in texture, ranging from silty clay loam (A horizon) to loam (C1 horizon). The *n*-value in AC horizons was > 7 and the clay percentage was > 8%. The *S. perennis* soil profile has lithological discontinuities because soil evolution was affected by temporal sea level transgression-regression between the gravel beach ridge and the sandy loam–sandy intertidal. The horizon suffix "o" was considered in this study to indicate residual accumulation of pedogenic sesquioxides (Schoeneberger *et al.*, 2012). The genesis of these redox concentrations in the 4Co horizon was conditioned by the more porous gravel and sand deposit and aerated than the overlying sandy loam 3Cg horizon (depletion redox, soil color chroma 2). However, the Eh values in both horizons are similar, indicating that at the time of measurement, the 3Cg horizon was drained and already depleted in iron oxide when this horizon was reduced during past flooding (Lindbo *et al.*, 2010).

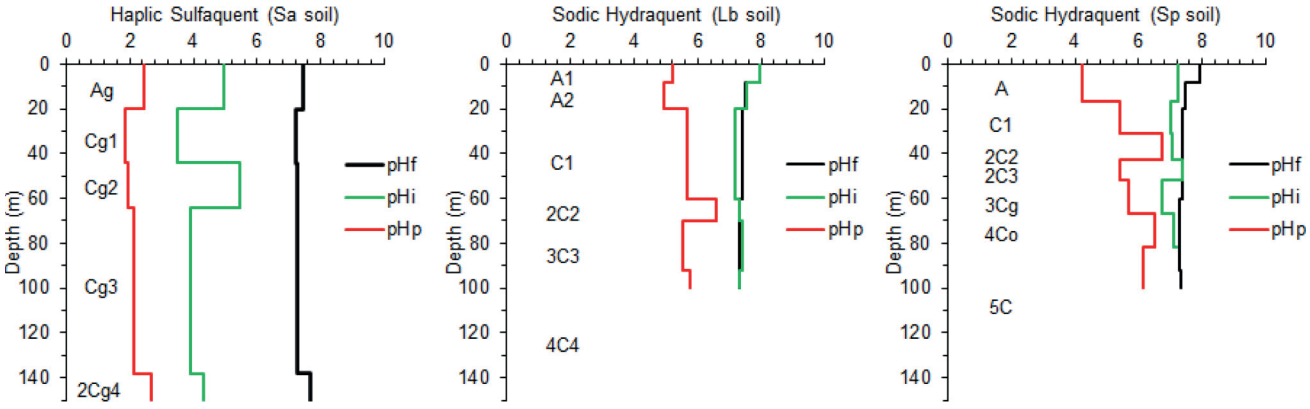

Figure 6. Field, incubation, and oxidation pH determinations. pHf: field pH, pHi: incubation pH, pHp: peroxide pH.

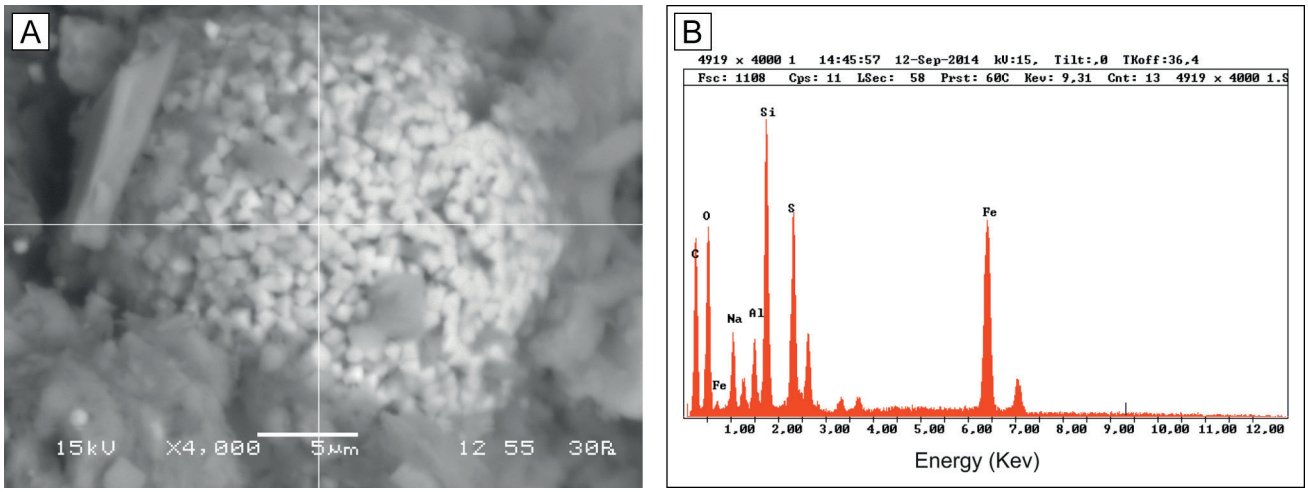

Figure 7. Sulfidic materials: a) Framboidal pyrites from Riacho salt marsh. b) EDS spectrum on octahedral pyrite.

Chemical properties

The chemical properties of the soil solution are shown in Tables 1 and 2. The field pH (pHf) varies between neutral to moderately basic (6.6 to 7.3), except in the A1 horizon of the Lb soil, which is basic (7.9). After incubation treatment, differences between pHf and pHi of 2 orders of magnitude were observed only in Sa soil, where this pH test indicates the occurrence of the sulfidic material, mainly pyrite (Fig. 6). SEM images showed pyrite framboids (Fig. 7a), where the EDS spectrum indicates the 2S:1Fe atomic ratio (Fig. 7b). Framboids comprise spheroidal aggregates with diameters varying between 5 to 30 μm, while octahedral pyrite microcrystals vary between 0.2 to 2 μm.

A marked peroxide pH (pHp < 4) reached some values of pHp 1.9 (Cg1 and Cg2) (Fig. 6). On the other hand, the pH values in the soil-water extract 1:2.5 maintained values slightly more acidic than the field pH (Table 2). There were differences in Eh values of the studied soils. Because of permanent waterlogging conditions (low marsh), the Sa soil reaches the lowest one (Eh<0), while Sp and Lb soils are the highest ones (Eh>0).

The Sa soil had a greater concentration of soluble salts, although all soil horizons have EC higher than 4 dSm^{-1} (except in 5C from Sp soil) and an ESP greater than 15%. Like Na^+, Cl^- was the dominant anion in soil solutions, and the molar ratio SO_4^{2-}/Cl^- was lower than 0.1 except in Ag-Cg1 horizons from Sa soil, C1-2C2-3C3 horizons from Lb soil and, A, 3Cg-4Co from Sp soil. In general, the highest CEC values were found in surficial and sub-surficial A-C horizons, like soil organic carbon and clay contents. The lower value of this property was registered in

Pedons	Depth	pH	EC	Na^+	K^+	Ca^{2+}	Mg^{2+}	SO_4^{2-}	Cl^-	SO_4^{2-}/Cl^-	ESP	CEC
Horizons	(cm)	1:2.5	(dSm^{-1})	($meql^{-1}$)							(%)	($cmolkg^{-1}$)
(Sa)				*Spartina alterniflora* soil, Haplic Sulfaquents								
Ag	0-20	6.36	90.2	521.7	12.3	153.9	42.2	167.0	680.0	0.25	77.2	52.2
Cg1	20-44	5.85	92.0	492.8	10.2	111.7	88.9	226.5	683.0	0.33	72.0	52.2
Cg2	44-64	6.70	117.1	637.7	12.8	222.3	37.6	34.5	928.0	0.04	82.1	52.2
Cg3	64-138	6.13	52.7	384.1	2.9	120.7	22.2	62.8	559.0	0.11	66.4	51.3
2Cg4	>138	6.98	17.4	119.6	2.6	42.1	6.2	1.2	154.6	0.01	35.0	11.7
(Lb)				*Limonium brasiliense* soil, Sodic Hydraquents								
A1	0-8	7.84	15.6	58.7	1.3	16.6	3.0	3.6	135.6	0.03	26.7	60.0
A2	8-20	7.61	12.6	102.2	1.7	15.4	2.7	4.5	113.1	0.04	49.3	48.7
C1	20-60	7.38	13.3	100.0	1.6	12.9	2.9	29.2	113.9	0.26	51.8	42.6
2C2	60-70	7.51	6.3	52.2	1.1	6.2	1.9	15.1	52.3	0.29	37.4	8.7
3C3	70-92	7.36	5.8	37.0	0.8	5.8	1.3	12.6	48.3	0.26	28.0	10.9
4C4	>92	7.25	5.3	37.0	0.6	4.8	1.5	11.3	44.9	0.25	29.8	7.0
(Sp)				*Sarcocornia perennis* soil, Sodic Hydraquents								
A	0-17	6.92	24.7	147.8	2.6	42.2	6.4	53.4	225.7	0.24	43.4	57.4
C1	17-31	7.07	9.0	99.6	2.1	21.2	2.7	8.5	134.2	0.06	41.6	28.7
2C2	31-43	7.05	7.9	52.5	1.2	8.7	2.3	5.8	66.2	0.09	32.2	10.9
2C3	43-52	7.07	5.0	23.6	0.4	7.5	4.8	2.2	40.4	0.05	12.9	6.4
3Cg	52-67	6.79	9.4	58.0	1.0	6.8	5.9	20.4	81.7	0.25	32.9	18.4
4Co	67-82	7.06	15.1	32.6	0.6	4.3	4.1	11.2	42.0	0.27	22.4	7.3
5C	>82	7.46	1.5	8.3	0.2	2.6	1.5	0.7	11.7	0.06	7.3	2.3

Table 2. Chemical composition of soil solutions from Riacho salt marsh.

the 5C horizon of Sp soil. The equivalent carbonate weight in all the studied soils was less than 1%, and soil organic carbon and total nitrogen contents decreased in depth in all studied soil profiles.

Stable Carbon isotope analysis of soil organic matter and C/N values

The C/N ratio in the studied soils varied between 12.9 and 20.9, except in the C1 horizon of the Sp soil, where de C/N ratio value was 3.2 (Fig. 8, Table 1).

The isotope composition of soil organic carbon ($\delta^{13}C$) varied between -14.3 ‰ and -22.2 ‰ (Table 1). The organic matter in the Sp and Lb soils, which are located in the high marsh, exhibited more depleted values of $\delta^{13}C$ compared to the Sa soil found in the low marsh. Conversely, the Sa soil recorded the most enriched values of $\delta^{13}C$.

Asymmetric profiles both of the composition of δ13C and C4/C3 relative abundance are also observed in depth (Fig. 9). The upper part of the profile exhibits a sharp maximum in C4/C3 relative abundance (more depleted in δ13C) in the Sp soil which tails off down the profile, while in Lb and Sa soils, this relative abundance tends to increase again in depth. Furthermore, the isotope composition of leaf plant tissues of *S. alterniflora*, *L. brasiliense*, and *S. perennis* was measured as -14.4‰, -28.8‰, and -25.6‰, respectively.

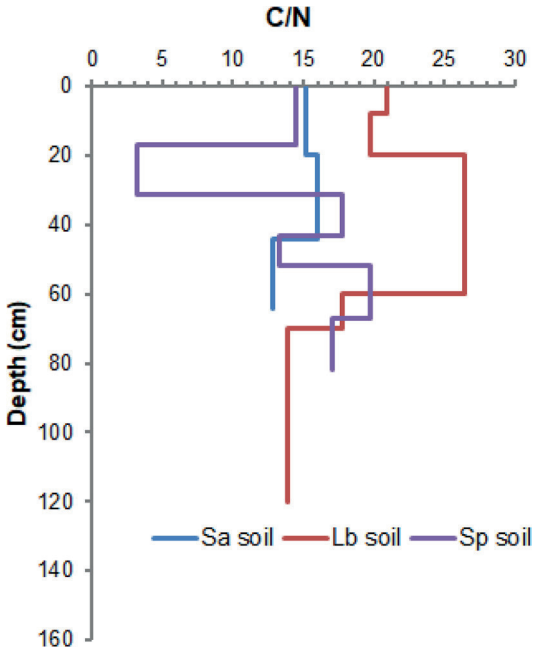

Figure 8. C/N ratio from soil organic matter in depth.

DISCUSSION

Geomorphology-soil relationships

The complex beach-ridge systems (spit systems) could not be formed by the typical drift currents bay but by turbulent fluxes generated due to the interaction of tidal currents over the shallow coastal topography as suggested by Bogazzi *et al*. (2005). These eddies are circular currents evidential by turbulent fluxes seen as vortex dipoles. The formation of these patterns inside the Golfo San José is due to the tidal flow passing through the narrow mouth of the gulf (Gagliardini, 2011). The analysis of Sentinel-2 satellite images (Fig. 10) showed that the gulf is divided into two domains, where the turbulent flux (vortex dipoles) was restricted to the west one (Amoroso and Galliardini, 2010). Presumably, it would be the cause of the formation of beaches-ridge systems during the regression after the transgressive stage of Holocene Climate Optimum (HCO) or Hypsithermal (ca. 9/8-6 ky, Aguirre *et al*., 2008).

According to the morphological characteristics and the lack of diagnostic horizons, the soils developed between beach-ridge systems correspond to the Entisols Order and due to the moisture regime conditions to the Aquents Suborder. The soils were also classified as saline-sodic because the EC> 4 dSm^{-1} and the ESP > 15%. (U.S. Salinity Laboratory Staff, 1954). The higher Ca^{2+}/Mg^{2+} ratio and a higher K^+ content detected in Sa soils could indicate a salt enrichment zone due to the periodic water table fluctuations (Dacey and Howes, 1984) or plants water uptake (i.e., evapotranspiration, Alvarez *et al*., 2015). The slight decreases of pH 1:2.5 soil-water extract could be due to acid sulfuric generation by oxidation of sulfidic materials during air drying of samples. This process can be observed by the SO_4^{2-}/Cl^- ratio, which is 0.1 in seawater from the Golfo San José (Alvarez *et al*., 2015).

Based on the aforementioned characteristics, as well as on the determination of n-values, the soils can be classified as Sodic Hydraquents for Sp and Lb soils, while Sa soils with identified sulfidic materials were classified as Haplic Sulfaquents (Soil Survey Staff, 2014).

The sulfidic material occurrence in Sa soil,

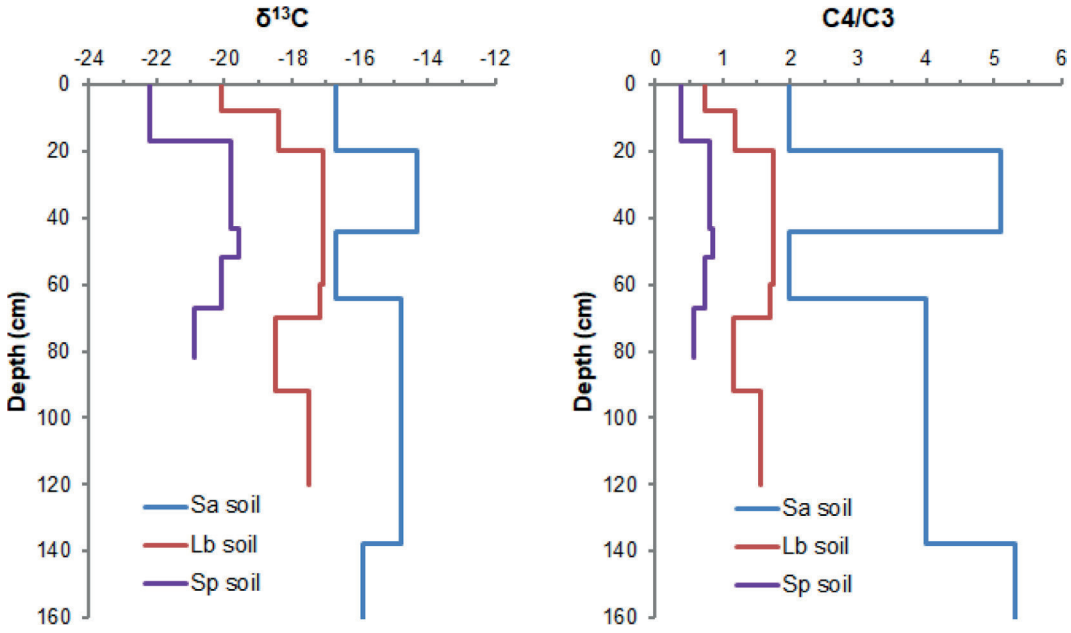

Figure 9. Isotope carbon composition ($\delta^{13}C$) and plant photosynthesis pathway proportion (C3 and C4) in the soil organic matter in depth.

composed mainly of pyrite framboids, is favored by anaerobic bacteria (sulfate-reducing bacteria) activity in fine sediments (DeFlaun and Mayer, 1983) in combination with the decomposition of organic matter produced in the *Spartina alterniflora* rhizosphere promoting both the sulfate reduction rate and the pyrite formation rate (Nie *et al.*, 2009). Pyrite framboids detected in permanently flooded soil were formed during the early diagenesis of the sediments (Giblin, 1988), and constitute a proxy to identify former Holocene salt marshes and coastal lagoons (Ferreira *et al.*, 2015; Osterrieth *et al.*, 2016).

Comparing the pH tests both in Table 1 and Figure 6 can see that inhibition of pyrite oxidation during incubation could be due to their buffering properties, such as high soil cation-exchange capacity (CEC) from clay minerals and/or by organic matter or due to the formation of coatings of iron and aluminum oxy-hydroxides and silica (Zhang and Evangelou, 1998; Bouza *et al.*, 2019). The hydrogen peroxide treatment could produce a breakdown of the buffering mechanism (Van Breemen, 1982, 1985). After peroxide oxidation treatment, the soil Sa was classified as potential acid sulfate soil (Ahern, *et al.*, 1998).

Usually, the degree of chemical reduction increases in depth in soils with a shallow water table, but this is not the case in soils with contrasting textures. The inversions of the Eh values processes detected in Sa soil were produced by the redox concentrations (Vepraskas *et al.*, 1993) either by aerated root (rhizoconcretions) in the Cg1 saturated horizon or by the abrupt textural change in the 2Cg4 horizon (pore size discontinuity) given by the presence of gravels (buried beach-ridges). In these aerated stratified gravel deposits, differences in nitrogen and phosphate were previously reported by Esteves and Varela (1991).

Soil-vegetation relationships on the isotope composition

The soil organic carbon predominantly originates from autochthonous C3 and C4 vascular vegetation, which indicates a terrestrial source. This is supported by the C/N ratio >12 in most horizons, indicating high levels of lignin, cellulose, and humic substances (Lamb *et al.*, 2006; Devesa-Rey and Barral, 2011). However, the low C/N ratio observed in the C1 horizon of the Sp soil may be attributed to the influence of organic matter derived from allochthonous marine sources, such as phytoplankton. Allochthonous organic matter typically contains higher nitrogen content (Tyson, 1995).

The provenance of C4 plants (most enriched values in $\delta^{13}C$) in low marsh level was derived

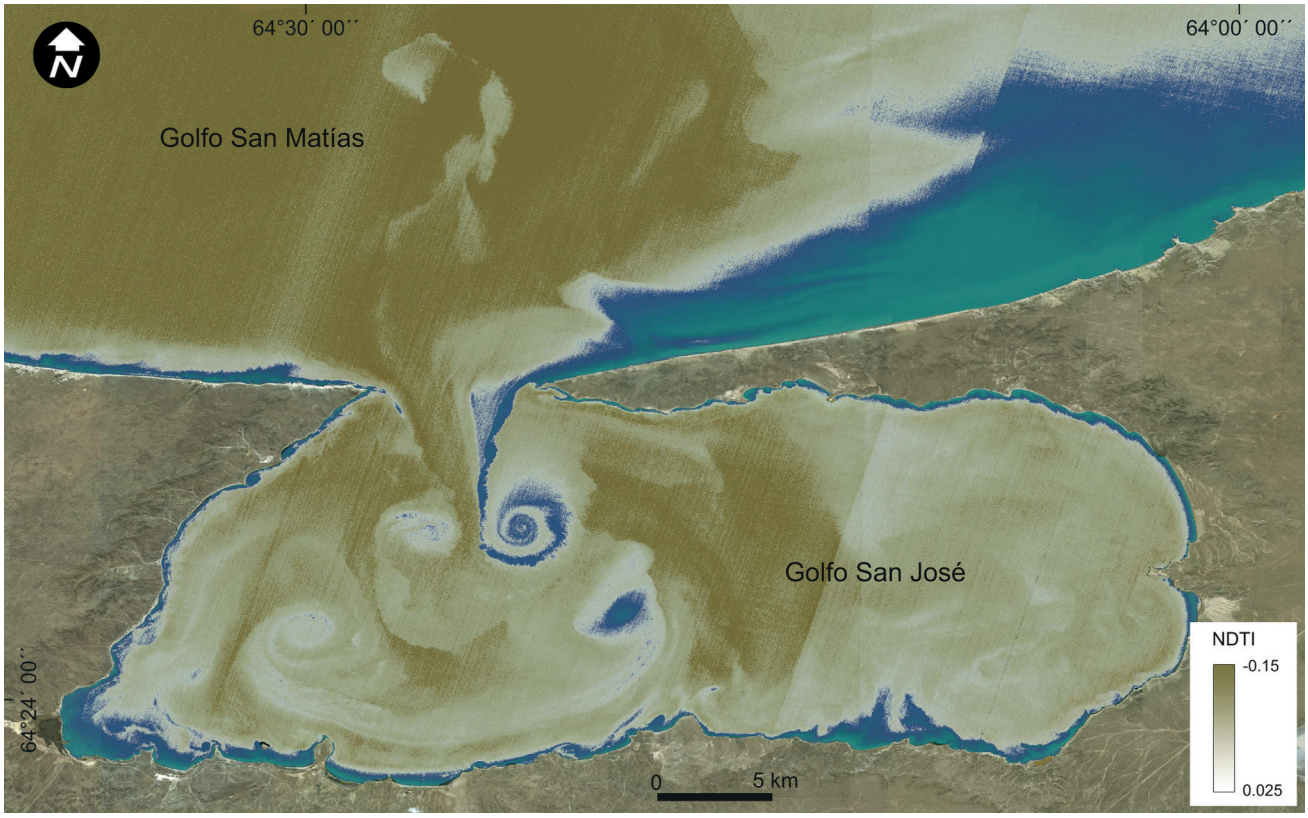

Figure 10. Sentinel-2 satellite image from March 22, 2022, with a resolution of 20 m per pixel. The patterns of suspended sediments as indicators of turbulent flows are observed (vortex dipoles).

from soil organic matter from *Spartina alterniflora* (Sa soil). In contrast, the provenance of C3 plants (more depleted values in $\delta^{13}C$) was derived from soil organic matter from *Limonium brasiliense* and *Sarcocornia perennis* (Lb and Sp soils) at high marsh levels. However, the presence of isolated patches of *Spartina densiflora*, typical of high salt marsh, could be interfering with these determinations since the isotopic values corresponding to genus *Spartina* are practically the same for both species found in this marsh but in different topographies. In these high salt marsh soils, the $\delta^{13}C$ enrichment at depth (Fig. 9) could indicate a possible assemblage of C4 plants when colonizing the old intertidal levels. That is, the originally installed vegetation could be *Spartina alterniflora*, constituting a pioneer marsh when sand and gravel C horizons at depth would have been a low tide area associated with beach ridge deposits (Figure 11). However, fluctuations in the $\delta^{13}C$ values (C4/C3) observed (Fig. 9) could be due to contributions of soil organic matter from C3 plants of continental ecosystems transported by surface runoff.

According to Ríos (2015), the total accretion rate in the Riacho marsh was determined to be 1.46 mm/yr. Based on the dominance of C4 plants at a depth of approximately 70 cm, it can be inferred that a C4 plant was present in the area around 470 years before present (BP). Similarly, in the Fracasso marsh located 40 km to the east, Ríos *et al*. (2018) estimated an accretion rate of 1.04 mm/yr in C horizons between 40 and 75 cm depth. These accretion rates, although influenced by sediment inputs from continental sources, are consistent with the hypothesis proposed by Bortolus *et al*. (2015) regarding the colonization of Spartina alterniflora. According to their findings, there are no historical records of the presence of *Spartina alterniflora* on the South American Atlantic coast until approximately two to three centuries ago.

CONCLUSIONS

Based on the results obtained in this contribution, it was determined that in Riacho salt marsh area, the complex beach-ridge systems (spit systems) would be formed by turbulent fluxes generated by the

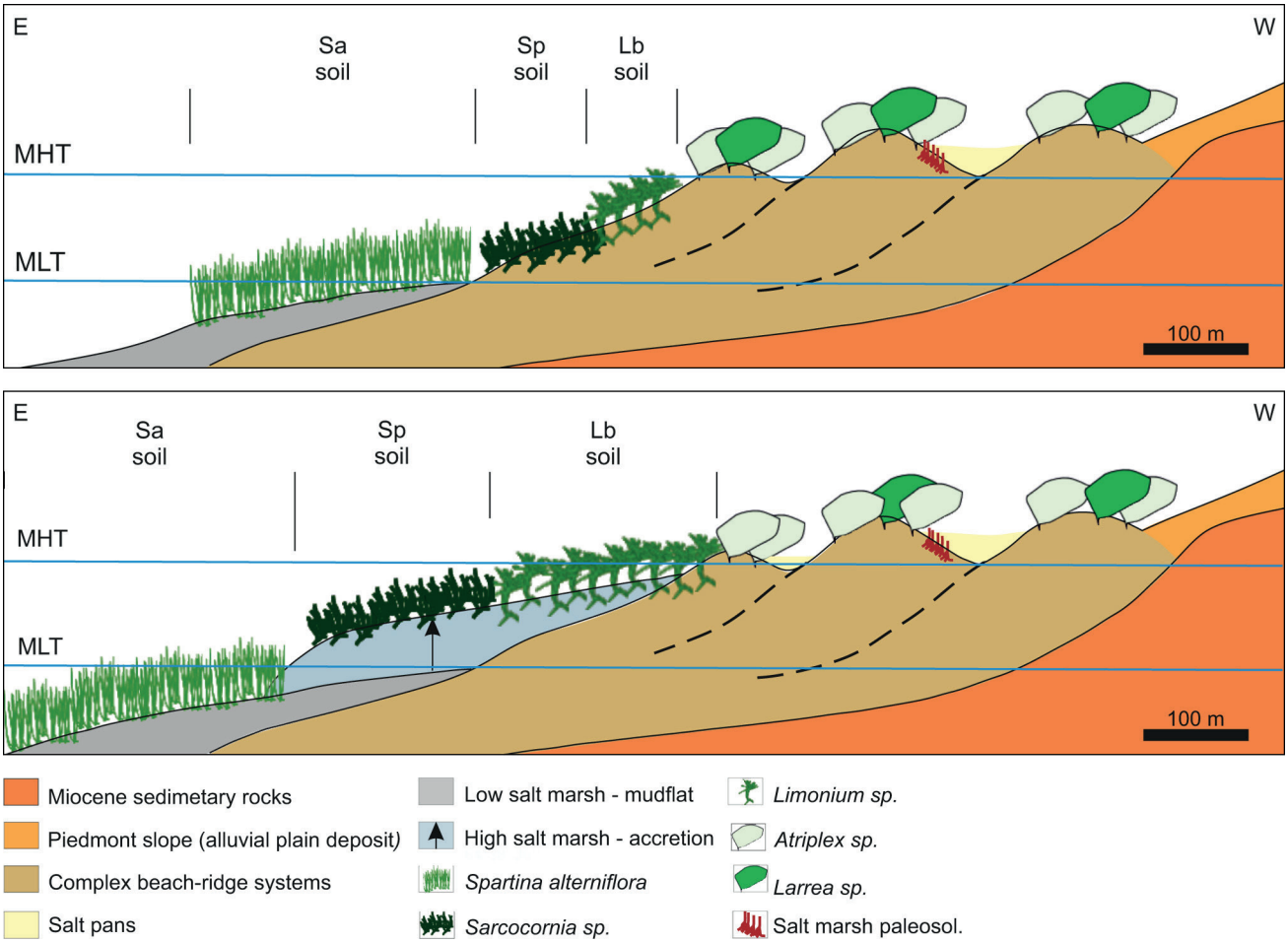

Figure 11. Possible soil–plant relationship and geomorphic evolution of Riacho salt marsh. MHT: mean high tide level; MLT: mean low tide level.

interaction of tidal currents over the shallow coastal topography (vortex dipoles).

The soils were classified as Sodic Hydraquents in high salt marshes positions corresponding to old intertidal areas developed between beach-ridges systems, dominated by *Sarcocornia perennis* and *Limonium brasiliense* (Sp and Lb soils, respectively), and Haplic Sulfaquents in low salt-marsh positions with *Spartina alterniflora* (Sa soil) corresponding to present-day intertidal plains. Sa soil was also considered potential acid sulfate soil because of the presence of oxidizable sulfide materials (pyrite). Oxidation processes in these soils (Eqs. 2 and 3) produce metal release (*e.g.*, iron and aluminum), which are considered phytotoxic. Given the drastic consequences for biota is mandatory to continue with the identification and mapping of potential acid sulfate soils to develop management and conservation strategies for these critical environments.

Concerning salt marsh landscape evolution, our results on $\delta^{13}C$ isotope compositions and the C/N ratio indicate that the sandy C horizons from Sp and Lb soils correspond to ancient or pioneer salt marsh, which is consistent with the Holocene salt marsh development. Nevertheless, even though there are accretion rate estimations, studies such as ^{14}C radiocarbon dating on soil organic matter (*e.g.*, accelerator mass spectrometry) should be done to establish more precisely when these processes occurred.

The zonation model is tested in response to ecological succession in combination with geomorphology, soils, and vegetation. However, fluctuations in the depth of C4/C3 ratios could be due to contributions from surface runoff of organic matter from C3 plants in continental ecosystems, so future isotopic studies from different sources will be necessary.

Acknowledgments

The authors would like to express their gratitude to Nilda Weiler, Claudia Sain, Lina Videla, and Estela Cortés for their important assistance during fieldwork and laboratory work, and to Professor Dra. Perla Imbellone and Dra. Natalia Borrelli who provided a valuable review of the original manuscript. This study was partially supported by the doctoral thesis of Ileana Ríos (2015) and the research project PICT 2018 03802 (FONCyT, Agencia Nacional de Promoción Científica y Tecnológica).

REFERENCES

Adam, P. (1993). *Saltmarsh ecology*. Cambridge University Press, UK. 461 pp.

Ahern, C.R., Powell B. and Ahern, M.R. (1998). Guidelines for sampling and analysis of lowland acid sulfate soils (ASS) in Queensland. Department of Natural Resources, Resource Sciences Centre, Queensland Acid Sulfate Soils Investigation Team. *Indooroopilly*. 33 pp.

Aguirre, M.L., Hlebszevitsch Savalscky, J.C., and Dellatorre, F. (2008). Late Cenozoic Invertebrate Paleontology of Patagonia and Tierra del Fuego, with Emphasis on Molluscs. In: J. Rabassa, (Ed.), *The Late Cenozoic of Patagonia and Tierra Del Fuego*, Elsevier, 14: 285-326.

Alvarez, M.D.P., Carol, E., and Dapeña, C. (2015). The role of evapotranspiration in the groundwater hydrochemistry of an arid coastal wetland (Península Valdés, Argentina). *Science of The Total Environment*, 506: 299-307.

Álvarez-Rogel, J., Silla, R.O., and Ariza, F.A. (2001). Edaphic characterization and soil ionic composition influencing plant zonation in a semiarid Mediterranean salt marsh. *Geoderma*, 99: 81-98.

Amoroso, R.O., and Gagliardini D.A. (2010). Inferring complex hydrographic processes using remote-sensed images: turbulent fluxes in the Patagonian gulfs and implications for scallop metapopulation dynamics. *Journal of Coastal Research*, 26: 320-332.

Bertness, M.D., and Shumway, S.W. (1993). Competition and facilitation in marsh plants. *The American Naturalist*, 142: 718-724.

Bocco, G., Cinti, A., and Urquijo, P. (2013). La construcción social del paisaje en comunidades de pescadores artesanales. El caso de la Península de Valdés, provincia del Chubut, Argentina. *Biblio 3w: Revista Bibliográfica de Geografía y Ciencias Sociales*, Vol. XVIII, Nº 1012.

Bogazzi, E., Baldoni, A., Rivas, A., Martos, P., Reta, R., Orensanz, J.M., Lasta, M., Dell P'Arciprete, P., and Werner, F. (2005). Spatial correspondence between areas of concentration of Patagonian scallop (*Zygochlamys patagonica*) and frontal systems in the southwestern Atlantic. *Fisheries Oceanography*, 14(5): 359–376

Bortolus, A. (2006). The austral cordgrass *Spartina densiflora* Brong.: its taxonomy, biogeography and natural history. *Journal of Biogeography*, 33: 158-168.

Bortolus, A., Schwindt, E., Bouza, P.J., and Idaszkin, Y.L. (2009). A characterization of Patagonian salt marshes. *Wetlands*, 29: 772-780.

Bortolus, A., Carlton, J.T., and Schwindt, E. (2015). Reimagining South American coasts: unveiling the hidden invasion history of an iconic ecological engineer. *Diversity and Distributions*, 21: 1267-1283.

Bortolus, A., Adam, P., Adams, J.B., Ainouche, M.L., Ayres, D., Bertness, M.D., Bouma, T.J., Bruno, J.F., Caçador, I., Carlton, J.T., Castillo, J.M., Costa, C.S.B., Davy, A.J., Deegan, L., Duarte, B., Figueroa, E., Gerwein, J., Gray, A.J., Grosholz, E.D., Hacker, S.D., Hughes, A.R., Mateos-Naranjo, E., Mendelssohn, I.A., Morris, J.T., Muñoz-Rodríguez, A.F., Nieva, F.J.J., Levin, L.A., Li, B., Liu, W., Pennigs, S.C., Pickart, A., Redondo-Gómez, S., Richardson, D.M., Salmon, A., Schwindt, E., Silliman, B.R., Sotka, E.E., Stace, C., Sytsma, M., Temmerman, S., Turner, R.E., Valiela, I., Weinstein, M.P., and Weis, J.S. (2019). Supporting *Spartina*: Interdisciplinary perspective shows *Spartina* as a distinct solid genus. *Ecology* 100: e02863. https://doi.org/10.1002/ecy.2863

Boschi, E.E. (1979). Geographic distribution of Argentinian marine decapods crustaceans. *Bulletin of the Biological Society of Washington*, 3: 134-143.

Boutton, T.W. (1991). Stable carbon isotopes ratios of soil organic matter and their use as indicators of vegetation and climate change. In: T.W. Boutton and S.I. Yamasaki (Eds.), *Mass Espectrometry of Soils*. Marcel Dekker, New York, 2: 47–82.

Bouyoucos, G.W. (1927). The hydrometer as a new method for the mechanical analysis of soils. *Soil Science*, 23: 343-353.

Bouza, P.J., Ríos, I., Idaszkin, Y.L., and Bortolus, A. (2019). Patagonian salt marsh soils and oxidizable pedogenic pyrite: solid phases controlling aluminum and iron contents in acidic soil solutions. *Environmental Earth Sciences*, 78, 1-14.

Bouza, P.J., Sain C.L., Bortolus, A., Ríos, I., Idaszkin, Y.L., and Cortés, E.G. (2008). *Geomorfología y características morfológicas y fisicoquímicas de suelos hidromórficos de marismas patagónicas*. XXI Congreso Argentino de la Ciencia del Suelo. Actas: 450, Potrero de los Funes, San Luis.

Cabrera, A.L. (1976). Regiones fitogeográficas argentinas. Enciclopedia Argentina de Agricultura y Jardinería (2nd. Ed.). Tomo n, Fase l. ACME, Buenos Aires. 85 pp.

Carvajal, A.F., Feijoo, A., Quintero, H., and Rondón, M.A. (2013). Soil organic carbon storage and dynamics after C3-C4 and C4-C3 vegetation changes in sub- Andean landscapes of Colombia. *Chilean Journal of Agricultural Research*, 73: 391-398.

Chmura, G., and Aharon, P. (1995). Stable carbon isotope signatures of sedimentary carbon in coastal wetlands as indicators of salinity regime. *Journal of Coastal Research*, 11: 124–135

Choi, Y., Wang, Y., Hsieh, Y.P., Robinson, L. (2001). Vegetation succession and carbon sequestration in a coastal wetland in northwest Florida: evidence from carbon isotopes. *Global Biogeochemical Cycles*, 15: 311–319.

Coronato, F.R. (1994). Clima del nordeste del Chubut. *Séptima Reunión de Campo del Comité Argentino para el Estudio del Cuaternario (CADINQUA)*. Puerto Madryn, Argentina: CENPAT-CONICET, 13-20.

Coronato, F.R., Pessacg, N., and Alvarez, M.P. (2017). The Climate of Península Valdés within a regional frame. In: P.J. Bouza and A. Bilmes (Eds.), *The Late Cenozoic of Península Valdés, Patagonia, Argentina: an interdisciplinary approach*. Springer Earth System Sciences, 4: 85-104.

Committee on Characterization of Wetlands. (1995). *Wetlands: characteristics and boundaries*. National Research Council. 328 pp.

Coplen, T.B., Brand, W.A., Gehre, M., Gröning, M., Meijer, H.A., Toman, B., and Verkouteren, R.M. (2006). New guidelines for $\delta^{13}C$ measurements. *Analytical Chemistry*, 78: 2439-2441.

Dacey, J.W., and Howes, B.L. (1984). Water uptake by roots controls water table movement and sediment oxidation in short *Spartina* marsh. *Science*, 224: 487-489.

Davies, B.E. (1974). Lost on ignition as an estimate of soil organic matter. *Soil Science*, 38: 150 -151.

DeFlaun, M.F., and Mayer, L.M. (1983). Relationships between bacteria and grain surfaces in intertidal sediments. *Limnology and Oceanography* 28(5): 873–881.

Devesa-Rey, R., and Barral, M.T. (2011). Allochthonous versus autochthonous naturally occurring organic matter in the Anllóns river bed sediments (Spain). *Environmental Earth Science*, 66: 773–782.

Ehleringer, J.R., and Cerling, T.E. (2002). C3 and C4 photosynthesis. *Encyclopedia of Global Environmental Change*, 2: 186-190.

Esteves, J.L., and Varela, D.E. (1991). Dynamics of nutrient cycling of the Valdes Bay-Punta Cero pond system (Peninsula Valdés, Patagonia) Argentine. *Oceanologica Acta*, 14: 51-58.

Farquhar, G.D., Ehleringer, J.R., and Hubick, K.T. (1989). Carbon isotope discrimination and photosynthesis. *Annual Review of Plant Physiology and Plant Molecular Biology,* 40: 503–537.

Faulkner, S., Patrick, W., and Gambrell, R. (1989). Field techniques for measuring wetland soil parameters. *Soil Science Society of America Journal*, 53: 883–890.

Ferreira, T.O., Nóbrega, G.N., Albuquerque, A.G.B.M., Sartor, L.R., Gomes, I.S., Artur, A.G., and Otero, X.L. (2015). Pyrite as a proxy for the identification of former coastal lagoons in semiarid NE. Brazil. *Geo-Marine Letters*, 35: 355–366

Gagliardini, D.A. (2011). Medium resolution microwave, thermal and optical satellite sensors: characterizing coastal environments through the observation of dynamical processes. In: D. Tang (ed.), *Remote Sensing of the Changing Oceans*, DOI 10.1007/978-3-642-16541-2_13.

Giblin, A.E. (1988). Pyrite formation in marshes during early diagenesis. *Geomicrobiology Journal*, 6: 77-97.

Haller, M.J. (2017). Geology of Peninsula Valdés. In: P.J. Bouza and A. Bilmes (Eds.), *The Late Cenozoic of Península Valdés, Patagonia, Argentina: an interdisciplinary approach*. Springer Earth System Sciences, 2: 23-46.

Haller, M.J. (1981). *Descripción geológica de la Hoja 43 h, Puerto Madryn, provincia del Chubut*. Servicio Geológico Nacional, Boletín, Buenos Aires, 184pp.

Idaszkin, Y.L., and Bortolus, A. (2011). Does low temperature prevent *Spartina alterniflora* from expanding toward the austral-most salt marshes? *Plant Ecology*, 212: 553-561.

Hattersley, P.W. (1983). The distribution of C3 and C4 grasses in Australia in relation to climate. *Oecologia* 57: 113–12.

Idaszkin, Y.L., Bortolus, A., and Bouza, P.J. (2011). Ecological processes shaping Central Patagonian salt marsh landscapes. *Austral Ecology*, 36: 59-67.

Idaszkin, Y.L., Bortolus, A., and Bouza, P.J. (2014). Flooding effect on the distribution of native austral cordgrass *Spartina densiflora* in Patagonian salt marshes. *Journal of Coastal Research*, 30: 59-62.

Idaszkin, Y.L., Lancelotti, J.L., Bouza, P.J., and Marcovecchio, J.E. (2015). Accumulation and distribution of trace metals within soils and the austral cordgrass *Spartina densiflora* in a Patagonian salt marsh. *Marine Pollution Bulletin*, 101: 457-465.

Idaszkin, Y.L., Alvarez, M.D.P., and Carol, E. (2017). Geochemical processes controlling the distribution and concentration of metals in soils from a Patagonian (Argentina) salt marsh affected by mining residues. *Science of the Total Environment*, 596: 230-235.

Lacaux, J.P., Tourre, Y.M., Vignolles, C., Ndione, J.A., and Lafaye, M. (2007). Classification of ponds from high-spatial resolution remote sensing: application to rift valley fever epidemics in Senegal. *Remote Sensing of Environment*, 106: 66–74.

Laffoley, D., and Grimsditch, GD. (2009). *The management of natural coastal carbon sinks*. IUCN, Gland, Switzerland. 53 pp.

Lamb, A.L., Wilson G.P., and Leng M.J. (2006). A review of coastal palaeoclimate and relative sea-level reconstructions using $\delta^{13}C$ and C/N ratios in organic material. *Earth Science Review*, 75: 29-57.

Lamb, A.L., Vane, C.H., Wilson, G.P., Rees, J.G., and Moss-Hayes, V.L. 2007. Assessing $\delta^{13}C$ and C:N ratios from organic material in archived cores as Holocene sea level and palaeoenvironmental indicators in the Humber Estuary, UK. *Marine Geology*, 244: 109-128.

Leeuw, J., Munck, W., Olff, H., and Bakker, J.P. (1993). Does zonation reflect the succession of salt marsh vegetation? A comparison of an estuarine and a coastal bar island marsh in The Netherlands. *Acta botanica Neerlandica*, 42(4): 435-445.

Li, S.H., Ge, Z.M., Xie, L.N., Chen, W., Yuan, L., Wang, D.Q., Li, X.Z., and Zhang, L.Q. (2018). Ecophysiological response of native and exotic salt marsh vegetation to waterlogging and salinity: Implications for the effects of sea-level rise. *Scientific Reports*, 5; 8(1): 2441. doi: 10.1038/s41598-017-18721-z.

Lin, C., and Melville, M.D. (1993). Control of soil acidification by fluvial sedimentation in an estuarine floodplain, eastern Australia. *Sedimentary Geology*, 85: 271-284.

Lindbo, D., Stolt, M.H. and Vepraska, M. (2010). Redoximorphic features. In: G. Stoops, V. Marcelino, F. Mees (Eds.), *Micromorphological features of soils and regoliths. Their relevance for pedogenic studies and classifications*. Elsevier, 8: 129-147.

Menni, R.C., and Gosztonyi, A.E. (1982). Benthic and semidemersal fish associations in the Argentine Sea. *Studies on Neotropical Fauna and Environment*, 17:1-29.

Mitsch, W.J., and Gosselink, J.G. (2000). The value of wetlands: importance of scale and landscape setting. *Ecological Economics*, 35: 25-33.

Mitsch, W.J., and Gosselink, J.G. (1993). *Wetlands*. Van Nostrand Reinhold, New York. 722 pp.

Nellemann, C., Corcoran, E., Duarte, C.M., Valdés, L., De Young, C., Fonseca, L., and Grimsditch, G. (2009). *Blue Carbon: a rapid response assessment*. United Nations Environment Programme, GRID-Arendal. UNEP. Earth print.

Nie, M., Wang, M., and Li, B. (2009). Effects of salt marsh invasion by *Spartina alterniflora* on sulfate-reducing bacteria in the Yangtze River estuary, China. *Ecological Engineering*, 35:1804–1808.

Osterrieth, M.L., Borrelli, N., Álvarez, F., Nóbrega, G., Machado, W., Ferreira, T.O., Soares Freire, A., and Santelli, R. (2016). Biochemistry of iron associated with pyritization in Holocene marshes, Mar Chiquita, Buenos Aires, Argentina. *Environmental Earth Science*, 75: 672. doi: 10.1007/s12665-016-5506-8.

Page, A.L., Miller, R.H., and Keeny, D.R. (1982). *Methods of Soil Analysis. Part 2: Chemical and Microbiological properties*. Second edition. American Society of Agronomy, Madison, Wisconsin.

Pennings, S.C., and Callaway, R.M. (1992). Salt marsh plant zonation: the relative importance of competition and physical factors. *Ecology*, 73: 681-690.

Pye, K., and French, P.W. (1993). *Erosion and accretion processes on British Salt Marshes. Vol. 1, Introduction: Saltmarsh Processes and Morphology*. Cambridge Environmental Research Consultants, Cambridge.

Ríos, I. (2015). *Relaciones edafo-geomorfológicas y geo-ecología de plantas vasculares en marismas patagónicas: propiedades morfológicas, físicas, químicas y biogeoquímicas*. Ph.D. Thesis, Universidad Nacional de Córdoba. Córdoba, Argentina. 170 pp. (unpublished).

Ríos, I., Bouza, P.J., Bortolus, A., and Alvarez, M.P. (2018). Soil-geomorphology relationships and landscape evolution in a southwestern Atlantic tidal salt marsh in Patagonia, Argentina. *Journal of South American Earth Sciences*, 84: 385-398.

Schoeneberger, P.J., Wysocki, D.A., Benham E.C., and Soil Survey Staff. (2012). *Field book for describing and sampling soils, Version 3.0.* Natural Resources Conservation Service, National Soil Survey Center, Lincoln.

Soil Survey Staff. (1999). *Soil taxonomy. A basic system of soil classification for making and interpreting soil surveys; 2nd edition.* Agricultural Handbook 436. Natural Resources Conservation Service, USDA, Washington, 869 pp.

Soil Survey Staff. (2014). *Keys to Soil taxonomy, 12th ed.: A basic system of soil classification for making and interpreting soil surveys.* USDA-SCS Agric. Handbook. U.S. Gov. Printing Office, Washington, DC. 436 pp.

Tyson, R.V. (1995). *Sedimentary Organic Matter: Organic Facies and Palynofacies*. Chapman and Hall, Springer Science & Business Media. London, 615 pp.

U.S. Salinity Laboratory Staff. (1954). *Diagnosis and Improvement of Saline and Alkali Soils*, Handbook 60. U.S. Department of Agriculture, Washington, DC., 160 pp.

Van Breemen, N.V. (1982). Genesis, Morphology, and Classification of Acid Sulfate Soils in Coastal Plains. In: J.A. Kittrick, D.S. Fanning and L.R. Hossner (Eds.), *Acid sulfate weathering*. Soil Science Society of America, Special Publication No 10: 95-108.

Vepraskas, M., Wilding, L., and Drees, L. (1993). Aquic conditions for Soil Taxonomy: Concepts, soil morphology and micromorphology. *Developments in Soil Science* 22: 117-131. https://doi.org/10.1016/S0166-2481(08)70402-1

Weiler, N.E. (1998). Mid-Holocene Littoral Deposits at Southwest of the Golfo San Jose, Peninsula Valdes, Argentine Republic. *Journal of Coastal Research*, 26: 234-237.

Weiguo, L., Zisheng, A., Weijian, Z., Head, M.J., and Delin, C. (2003). Carbon isotope and C/N ratios of suspended matter in rivers: an indicator of seasonal change in C4/C3 vegetation. *Applied Geochemistry*, 18: 1241-1249.

White, I., Melville, M.D., Wilson, B.P., and Sammut, J. (1997). Reducing acidic discharges from coastal wetlands in eastern Australia. *Wetlands Ecology and Management*, 5: 55-72.

Zhang, Y.L., and Evangelou, V.P. (1998). Formation of ferric hydroxide-silica coatings on pyrite and its oxidation behavior. *Soil Science*, 163: 53–62.